Selective uptake of Ag(I) from aqueous solutions using ionic liquid modified iron oxide nanoparticles

Abiodun D. Aderibigbe[a*], *Richard A. Crane*[b,c], *Martin R. Lees*[d] *and Andrew J. Clark*[a]

[a] Department of Chemistry, University of Warwick, Coventry, CV4 7AL, United Kingdom

[b] Camborne School of Mines, College of Engineering, Mathematics and Physical Sciences, University of Exeter, Penryn Campus, Penryn, Cornwall, TR10 9FE. United Kingdom

[c] Environment and Sustainability Institute, University of Exeter, Penryn Campus, Penryn, Cornwall, TR10 9FE. United Kingdom

[d] Department of Physics, University of Warwick, Coventry, CV4 7AL, United Kingdom

Graphical Abstract

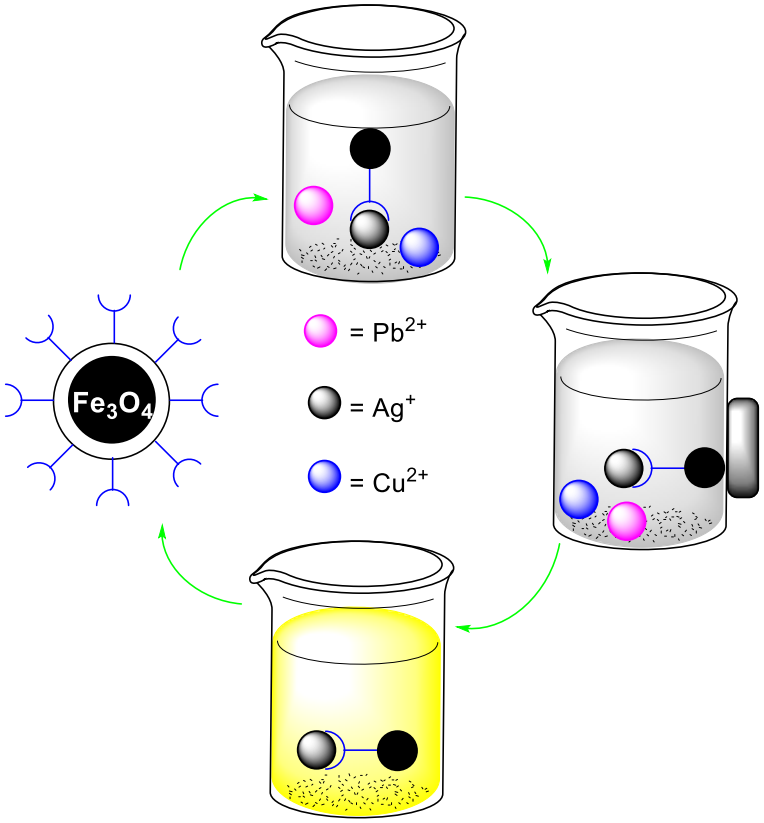

Abstract

Surface functionalized magnetic nanoparticles represent a potentially highly valuable tool for the selective recovery of metals from the aqueous phase, due to their ability to be manipulated and then recovered using an externally applied magnetic field. Ionic liquids are ideal candidates for such surface functionalization for a range of reasons, including

*Corresponding Author currently at: Chemistry Department, Federal University of Technology Akure, P.M.B. 704 Akure, Ondo state, Nigeria.

Current Email address: a.aderibigbe.1@warwick.ac.uk

their enhanced selectivity, low water consumption and high chemical stability. Herein the removal of Ag^+ onto $[MTESPIm]^+[Cl]^-$ on $Fe_3O_4@SiO_2$ as a function of pH, exposure time, nanosorbent concentration and type of stripping agent has been investigated. Ag^+ removal was recorded to fit the Langmuir isotherm indicating monolayer formation, with a saturation capacity of 23.69 mg/g. Moreover, optimum conditions for the selective removal of Ag^+ in preference to Cu^{2+} and Pb^{2+}, were recorded at pH 3, exposure time ranging between 0-15 min and with the highest nanosorbent concentration tested (80 mg/10ml of adsorbate solution). In addition, the most efficient stripping agent for the sorbed Ag^+ was determined to be thiourea at 0.6 M. Overall the results indicate that $[MTESPIm]^+[Cl]^-$ on $Fe_3O_4@SiO_2$ is a highly adaptable and efficient agent for the selective recovery of Ag from the aqueous phase.

Keywords: Selective silver recovery; ionic liquid; iron oxide nanoparticle; surface functionalization; soft donor.

Introduction

As the global population continues to expand, demand for modern products and services which use silver (Ag), including: electronic equipment, catalysis, antibacterial agents, jewelry, water filtration media, etc., will almost certainly continue to increase (Sahan et al. 2019; Taillades and Sarradin 2004; Butterman and Hilliard 2005). Moreover Ag is listed within the EU 27 critical raw materials, and currently exhibits an "end-of-life recycling input rate" of only ~14% (Butterman and Hilliard 2005). Therefore, in order to overcome this urgent and burgeoning problem new technology is required for the enhanced recovery of Ag from our waste materials and end-of-life products (Avarmaa et al. 2019). A key challenge associated with this, however, is that such waste is typically chemically complex and mixed with a wide range of ancillary metal(loids)/materials. It is therefore clear that the development of increasingly efficient, selective and cost-effective Ag^+ recovery process is highly beneficial.

To date, much research and development has been conducted on the removal of Ag ions from the aqueous phase including methods such as: solvent extraction (Daubinet and Kaye 2002) ion exchange (Virolainen et al. 2015) chemical precipitation (Ahlatcı et al. 2016) and solid phase extraction (Abdolmohammad-Zadeh and Javan 2015; Karimi et al. 2012). Solid phase removal media have often been preferred due to the simplicity of their application, their often low disposal costs, and often high removal efficacy (Abdolmohammad-Zadeh and Javan 2015). Within such applications, nanoparticles, defined as particles which exhibit at least one length <100nm, have received great interest due to their superior surface area and commensurate high reactivity with the aqueous phase. Such materials can also be utilized in various new applications due to their ability to be suspended in the aqueous phase as a colloid (e.g. subsurface injection). Magnetic nanoparticles have received particularly high interest due to their additional ability to be manipulated and then recovered from the aqueous phase using an externally applied magnetic field. Additional important properties for nanosorbents include stability across a wide pH range, high and rapid ion extraction efficacy, facile ion stripping efficacy and low synthesis cost. Nanosorbents possessing these desired properties have been reported. For example, in 2018, some researchers reported that the nanosorbent - $Fe_3O_4@SiO_2@TiO_2@$ Ag^+-imprinted 2,4-diamine-6-phenyl-1,3,5-triazine demonstrated a higher distribution ratio and selectivity coefficient than the non-imprinted analogue in the selective extraction and preconcentration of Ag^+ (Jalilian and Taheri 2018). The nanosorbent could also be easily separated by a magnet and recycled. Extraction efficiency, however, was reported as relatively low at acidic pH. The synthesis of a Ag^+ imprinted 3-

(triethoxysilyl)propane-1-thiol tethered to $Fe_3O_4@SiO_2@TiO_2$ was reported and it was determined that the nanosorbent exhibits relatively high selectivity, at room temperature, for Ag^+ from aqueous solutions also containing Li^+, Co^{2+}, Cu^{2+} and Ni^{2+}(Yin et al. 2017). The industrial scale synthesis of such nanosorbents, however, is likely to be expensive due to the requirement for ultrapure reagents.

To date, research output on the synthesis and application of nanosorbents for the industrial scale selective extraction and preconcentration of trace concentrations of Ag^+ remains in its infancy. Such preliminary work include the combination of 5-amino-2-thiol-1,3,4-thiadiazole and sodium dodecyl sulphate tethered by their condensation onto Fe_3O_4/Al_2O_3, which was reported to extract Ag^+ selectively, rapidly and quantitatively even in the presence of several order of magnitude greater concentrations of Zn^{2+}, Bi^{3+} and Pd^{2+}(Karimi et al. 2012). Other examples include $Fe_3O_4@SiO_2@$(1*E*,1'*E*)-1,1'-(pentane-1,5-diylbis(2,1-phenylene))bis(*N*-(3-(trimethoxysilyl)propyl)methanimine) which was recorded to selectively remove Ag^+ in preference to Pb^{2+} and Cu^{2+}(Banaei et al. 2015). Furthermore, 1-methyl-3-[(3-trimethoxysilyl)propyl] imidazolium chloride ($[MTMSPIm]^+[Cl]^-$) anchored onto $Mn_3O_4@SiO_2$ nanoparticles and demonstrated high selectivity, reusability and efficiency for extraction and preconcentration of ultratrace concentrations of Ag^+ (i.e. 60 ng/mL). A key shortcoming, however, was the fact that relatively high nanosorbent mass to sample volume ratios were required. The nanosorbent was also not ideally suited for magnetic recovery applications due to the significantly lower magnetization saturation of Mn_3O_4 compared to Fe_3O_4 (Ozkaya et al. 2008). Ionic liquids (ILs) are compounds composed only of ions and with outstanding properties including little or very low volatility, low melting point, thermal stability and tunable hydrophilicity/hydrophobicity (Zhou et al. 2012; Seddon, Stark, and Torres 2000).

Herein we have built on this work by combining the proven selectivity of $[MTESPIm]^+[Cl]^-$ for Ag^+ recovery with the superior magnetic responsiveness of $Fe_3O_4@SiO_2$ (Fig. 1) (Ozkaya et al. 2008). Whilst $Fe_3O_4@SiO_2@[MTESPIm]^+[Cl]^-$ has been synthesized and applied for various different applications (e.g. catalysis, medicine, printing (Qian et al. 2017; Sajjadifar, Zolfigol, and Tami 2019; Zhou et al. 2012; Yang et al. 2011; Wei et al. 2013; Azgomi and Mokhtary 2015; Garkoti, Shabir, and Mozumdar 2017)**)** to the best of our knowledge this is the first investigation into various parameters for the selective uptake of Ag^+. The aim of this work was therefore to investigate its behavior towards Ag^+ across a range of differential constraints (namely: pH, contact time, nanosorbent dose, Ag^+ recovery efficacy by different stripping agents) in order to understand Ag^+ removal kinetics and mechanisms and thereby determine optimal application conditions.

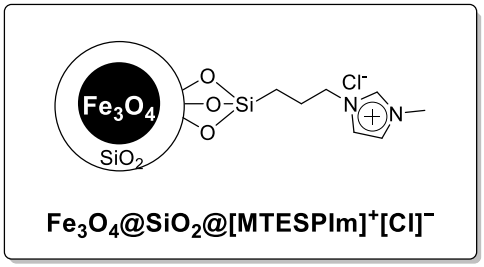

Fig. 1 Core-shell iron oxide/imidazolium-based Ag^+ nanosorbent composite nanosorbent ($Fe_3O_4@SiO_2@[MTESPIm]^+[Cl]^-$)

Experimental

Chemicals.

$FeSO_4.7H_2O$ (99%), $FeCl_3.6H_2O$ (97%), NH_4OH (25% v/v), Tetraethyl orthosilicate (99%), *N*-methylimidazole (99%), 3-Chloropropyltriethoxysilane (97%), thiourea (99%) and toluene (99.5%) were purchased from Sigma Aldrich, HCl (37%), HNO_3 (70%), $AgNO_3$ (99%), $NaNO_3$ (99%) and NaOH pellets (97%) were purchased from Fischer Scientific. $Cu(NO_3)_2.3H_2O$ (99%) and $Pb(NO_3)_2$ (99%) were purchased from Acros Chemicals. Ethanol absolute (99.8%) was purchased from VWR. All chemicals were used as received without further purification.

Equipment and characterization.

All ^1H and ^{13}C NMR spectra were recorded at room temperature on Bruker© Advance spectrometers. Fourier transform infra-red (FTIR) spectra were recorded on Bruker© Alpha Platinum-Attenuated Total Reflectance IR spectrometer. X-ray diffraction (XRD) data were collected on a Panalytical Empyrean X-ray diffractometer employing a Co Kα radiation at 40 kV and 40 mA. Transmission electron micrographs (TEM) were captured by means of the JEOL 2100+ machine operating an acceleration voltage of 200 kV from samples prepared on a copper EM grid. X-ray photoelectron spectroscopy (XPS) data were collected on the Kratos© AXIS Ultra DLD spectrometer and take off angle of 90° was used with Al(mono) x-ray source. Metal concentrations were measured by means of a PerkinElmer 5300DV Inductively Coupled Plasma Optical Emission spectrophotometer (ICP-OES). Thermogravimetry analyses (TGA) were undertaken by means of a Metler Toledo© DSC1 – STAR at a scan rate of 10 °C/min on samples placed inside 70 µL alumina pans under a nitrogen atmosphere from 25 – 900 °C. Magnetization data were recorded on a quantum design MPM S5S SQUID magnetometer at 300 K. Finally, the pH of the adsorbate solutions was monitored using the Hanna HI 8424 portable pH meter.

Synthesis of the ionic liquid immobilized on silica coated Fe_3O_4 nanoparticles.

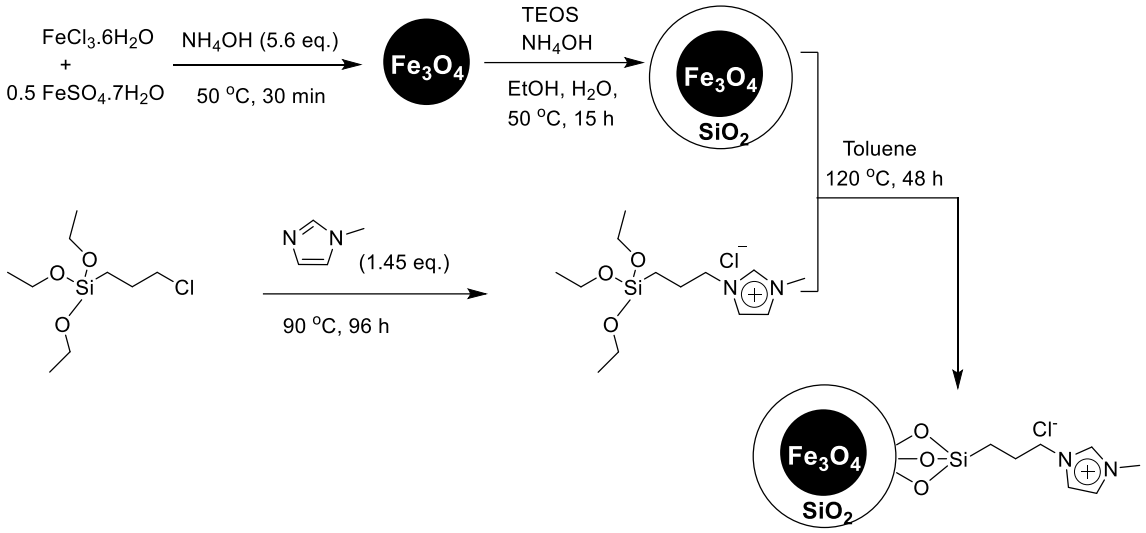

Scheme 1 Syntheses of the nanoparticles; Fe_3O_4 and $Fe_3O_4@SiO_2$, the ionic liquid; 1-methyl-3-[(3-triethoxysilyl)propyl] imidazolium chloride $[MTESPIm]^+$ $[Cl]^-$ and the ionic liquid-modified silica coated Fe_3O_4 nanosorbent.

The synthesis of the ionic liquid modified silica coated Fe_3O_4 nanosorbent was achieved over four steps (Scheme 1). In the first step, the magnetic core - Fe_3O_4 was prepared following the method previously reported (Naka et al. 2008). Briefly, $FeCl_3.6H_2O$ (5.41 g, 0.02 mole) and $FeSO_4.7H_2O$ (2.78 g, 0.01 mole) were dissolved by stirring in water (300 mL) at 50 °C. Then, NH_4OH (8.52 mL, 13.20 M, 0.11 mol) was added to the iron salts solution and vigorously stirred for 30 minutes, after which the black solids obtained were separated using a magnet. The solids were washed with water (100 mL x 3) and EtOH (50 mL x 3). Finally, the solids were dried *in vacuo* at 70 °C to give the black solid Fe_3O_4. In the second step, the silica coated Fe_3O_4 nanoparticle was prepared following the method previously reported (Fan et al. 2016). Briefly, to a stirred suspension of Fe_3O_4 (0.4 g) and TEOS (0.36 g) in dry EtOH (3 mL) at 50 °C was added a mixture of NH_4OH (0.66 mL, 13.20 M), EtOH (1.2 mL) and water (0.58 mL). The reaction was left to stir for 8 h at 50 °C and at the end of which the product suspension was left to cool to room temperature. The solids obtained were separated with a magnet, washed with water (25 mL x 3) and finally dried *in vacuo* at 70 °C to give $Fe_3O_4@SiO_2$ as a black solid. In the next step, the ionic liquid; 1-methyl-3-[(3-triethoxysilyl)propyl] imidazolium chloride ($[MTESPIm]^+[Cl]^-$) was accessed following a protocol previously reported (Abdolmohammad-Zadeh and Javan 2015). Hence, a mixture of *N*-methylimidazole (4.8 mL, 0.06 mol) and 3-chloropropyltriethoxysilane (9 mL, 0.04 mol) was refluxed at 90°C for 96 h, after which the crude product was left to cool to room temperature. This crude product was washed with dry diethyl ether (200 mL x 3) and dried *in-vacuo* at room temperature to give the ionic liquid; $[MTESPIm]^+$ $[Cl]^-$ as a light brown oil. Yield: 10.27 g (53 %), ^{1}H NMR (300 MHz, DMSO-d_6) δ 9.35 (s, 1H, NC*H*N), 7.80 (d, *J* = 6.0 Hz, 2H, NC*H*C*H*N), 4.16 (t, *J* = 6.5 Hz, 2H, CH_2CH_2N), 3.87 (s, 3H, CHNC*H*$_3$), 3.74 (q, *J* = 6.5 Hz, 6H, CH_3CH_2O), 1.81 (m, 2H, $CH_2CH_2CH_2$), 1.14 (t, *J* = 6.5 Hz, 9H, CH_3CH_2O), 0.51 (t, *J* = 6.5 Hz, 2H, $SiCH_2CH_2CH_2$). ^{13}C NMR (75 MHz, DMSO-d_6) δ 136.7 (NCHN) 123.6 (NCHCHN), 122.2 (NCHCHN), 57.8

130 ($CH_2\underline{C}H_2O$), 51.0 ($CH_3\underline{C}H_2N$), 35.7 ($CHN\underline{C}H_3$), 23.7 ($CH_2\underline{C}H_2CH_2$), 18.2 ($\underline{C}H_3CH_2O$), 6.7 ($Si\underline{C}H_3CH_3$), *m/z* (ESI)
131 $[M+Na]^+$ 348. Finally, a previously reported method was employed to prepare the ionic liquid ($[MTESPIm]^+$ $[Cl]^-$)
132 immobilized on the magnetic nanoparticle (Fe_3O_4@SiO_2) (Chen et al. 2014). Briefly, the Fe_3O_4@SiO_2 (1.5 g) was
133 dissolved in toluene (300 mL) and sonicated in an ultrasound bath at room temperature for 10 min. Meanwhile, the
134 ionic liquid (15.40 g) was dissolved in toluene (100 mL) and sonicated at room temperature for 10 min. The ionic
135 liquid solution was then added to the Fe_3O_4@SiO_2 and the mixture was refluxed at 120° C for 48 h. After 48 h, reaction
136 mixture was left to cool to room temperature and supernatant was decanted. The solid left behind was then washed
137 with deionized water (250 mL x 2) and EtOH (250 mL x 3) and finally dried *in vacuo* at 70°C to give the nanosorbent;
138 Fe_3O_4@SiO_2@$[MTESPIm]^+[Cl]^-$ as a brown solid.

139 Determination of particle diameter.

140 Particle diameter was evaluated using the Scherrer equation as defined below;

141 $$\tau = \frac{K\lambda}{\beta Cos\theta}$$

142 Where τ = particle diameter, K = Scherrer constant for spherical particles (0.94), λ = Wavelength of X-ray source, θ =
143 Bragg (diffraction) angle of the most intense peak and β = broadening at half the maximum intensity (FWHM) of the
144 most intense peak.

145 Determination of magnetic nanoparticle surface coverage.

146 The surface coverage of magnetic nanoparticle was evaluated using the equation defined below;

147 No of molecules per $nm^2 = \frac{W\ x\ d_{Fe_3O_4}\ x\ r\ x\ N_A}{M(1-W)\ x\ 3\ x\ 10^{21}}$

148 Where W is the weight loss of sample, d_{Fe3O4} is the density of the Fe_3O_4 = 5.17 g/cm^3, N_A is the Avogadro's constant
149 = 6.022 x 10^{23}, M is the molecular weight of the ligand, r is the radius of the composite nanoparticle.

150 Determination of sorption isotherms.

151 The sorption isotherm governing the removal of Ag^+ was predicted by means of three isotherms models - Langmuir,
152 Freundlich and Temkin using data generated from contacting the same amount (10 mg) of the nanosorbent with
153 varying Ag^+ concentrations (4 to 90 mgL^{-1}) at pH 3, for 15 mins at room temperature. Equations representing the
154 sorption isotherms are;

155 Langmuir isotherm:

156 $$\frac{C_e}{Q_e} = \frac{1}{Q_m\ K_L} + \frac{C_e}{Q_m}$$

157 Where C_e, Q_e, Q_m and K_L are the equilibrium Ag^+ concentration (mgL^{-1}), the amount of Ag^+ on the nanosorbent (mgg^{-1}), the maximum capacity of the nanosorbent (mgg^{-1}) and the Langmuir adsorption constant (L/mg) respectively.

Freundlich isotherm:

$$logQ_e = logK_F + \frac{1}{n} logC_e$$

Where Q_e and C_e have been described above, K_F and n are Freundlich constants related to maximum sorption capacity (mg/g) and heterogeneity factor (mg^{-1}).

Temkin isotherm:

$$Q_e = BlnA_T + BlnC_e$$

A_T (Lg^{-1}) and B ($Jmol^{-1}$) are Temkin constants related to the binding constant and heat of sorption respectively.

Ag^+ removal studies.

For the control study, a 500 mL aqueous solution containing 1 mgL^{-1} Ag^+ in 0.023 M $NaNO_3$ was prepared from a 500 mgL^{-1} stock solution. Afterwards, 20 mg of nanosorbents (Fe_3O_4, Fe_3O_4@SiO_2 and Fe_3O_4@SiO_2@$[MTESPIm]^+[Cl]^-$) were separately contacted with 10 mL of the Ag^+ aqueous metal solution at pH 1 inside 30 mL plastic screw cap vials. After 45 min the solids were magnetically separated in about 2 min and the supernatant was removed using a plastic syringe and prepared for metal content determination by ICP-OES. For the adsorption isotherm study, 10 mg of the nanosorbent (Fe_3O_4@SiO_2@$[MTESPIm]^+[Cl]^-$) was exposed to 10 mL aqueous solutions containing varying Ag^+ concentrations (4 to 90 mgL^{-1}) in 0.023 M $NaNO_3$ at pH 3 for 15 min. The batch experiments used to investigate the optimum conditions for the selective removal of Ag^+ onto Fe_3O_4@SiO_2@$[MTESPIm]^+[Cl]^-$ were conducted by exposing 10 mg of the nanosorbent to a 10 mL aqueous solution containing Cu^{2+}, Ag^+ and Pb^{2+} each at 2 mgL^{-1} in 0.023 M $NaNO_3$ at an initial pH of 3 unless otherwise stated. The pH of the metal aqueous solutions was adjusted to the desired pH using a few drops (typically between 1 and 10) of dilute 0.001M HNO_3 or NaOH. For initial pH study, pH of adsorbate solution was varied from 1 to 5. For the contact time study, contact time was varied from 0 to 90 mins. For nanosorbent dose study, amount of nanosorbent used was varied from 5 to 80 mg. All batch studies were undertaken in triplicates and at room temperature (21 ºC).

The metal removal efficiency was determined by the equation below;

$$\%\ RE = \frac{C_i - C_f}{C}\ X\ 100$$

Where *% RE* is percentage removal efficiency, C_i and C_f (in mgL^{-1}) are the initial and final metal ion concentrations respectively.

The selectivity factor was determined by the following equation (Shamsipur et al. 2014);

$$K_{Ag^+/M^{n+}} = \frac{K_d^{Ag^+}}{K_d^{M^{n+}}}$$

$$K_d = \frac{(C_i - C_f)v}{mC_f}$$

K_d is distribution ratio, C_i and C_f are initial and final metal ion concentration respectively (in mgL^{-1}), v is the volume of aqueous solution in mL, m is the mass of nanosorbent (in mg).

Ag^+ stripping efficiency studies.

For the stripping efficiency study, Ag^+-impregnated Fe_3O_4@SiO_2@$[MTESPIm]^+[Cl]^-$ nanosorbents were washed with de-ionized water and magnetically separated after which it was contacted with 5 mL of stripping agent (HCl, HNO or thiourea) inside screw-capped plastic vials for 1 h. Thereafter, the nanosorbent were magnetically separated and the supernatant stripping agent solution was carefully withdrawn using a plastic syringe. The stripping agent solution was made up to 10 mL by adding deionized water and the metal content was determined again by ICP-OES. The experiments were undertaken in triplicates. The stripping efficiency of Ag^+ by a stripping agent was determined following the equation;

$$\%SE = \frac{C_e}{C_i} X\ 100$$

Where *% SE* is percentage stripping efficiency, C_e represents the concentration of Ag^+ recovered by the stripping agent (Ag^+ concentration in the stripping agent solution) and C_i represents the initial Ag^+ concentration respectively (concentration of Ag^+ in nanosorbent prior to stripping).

Results and Discussion

Physical and chemical characterization of $[MTESPIm]^+[Cl]^-$ on Fe_3O_4@SiO_2.

The x-ray diffractogram of the black powder obtained after the treatment of $FeSO_4$ and $FeCl_3$ with aqueous ammonia is presented in Fig. 2. The experimental *d*-spacings from the x-ray diffractogram of the Fe_3O_4 are 2.96, 2.52, 2.09, 1.71, 1.61, 1.48 at 2θ (°) of 35.24, 41.58, 50.69, 63.24, 67.57 and 74.52 respectively. While the *d*-spacings are characteristic of Fe_3O_4 and identical to those reported in literature (Naka et al. 2008; Sun et al. 2007), the 2θ values are not, attributed to the difference in the x-ray sources used – Co Kα in this study but Cu Kα in the literature (Naka et al. 2008; Sun et al. 2007). The average diameter of the Fe_3O_4 particles evaluated by the Scherrer equation (Puig et al. 2012) was found to be 10.0±0.3 nm.

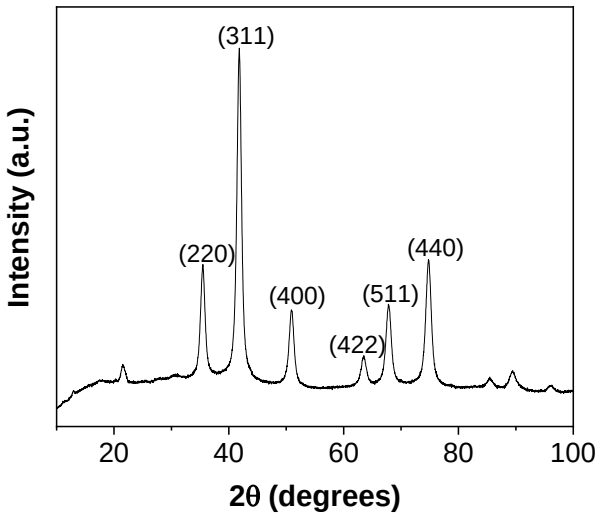

Fig. 2 X-ray diffractogram of Fe_3O_4 nanoparticles (Co Kα source wavelength = 1.79 Å, voltage = 40 kV, current = 40 mA)

The chemical composition of the different nanoparticles was each characterized using FTIR and XPS. FTIR spectra of all three nanoparticles (Fig. 3a) contain a peak around 554 cm^{-1} which was attributed to the Fe-O vibrations in Fe_3O_4 (Abbas et al. 2014). The spectrum for Fe_3O_4@SiO_2 also contained an intense peak at 1069 cm^{-1} (attributed to the Si-O-Si stretching vibrations) and suggesting that SiO_2 has been chemisorbed onto Fe_3O_4 (Abbas et al. 2014; Sajjadifar, Zolfigol, and Tami 2019). While the spectra of the Fe_3O_4@SiO_2 and the Fe_3O_4@SiO_2@$[MTESPIm]^+[Cl]^-$ may look identical, the low intensity peak at 1558 cm^{-1} (attributed to the -C=N stretching vibration) slightly differentiates them, indicating that the ionic liquid ($[MTESPIm]^+[Cl]^-$) may have been linked to the Fe_3O_4@SiO_2 (Minsik Kim, Hwang, and Yu 2007).

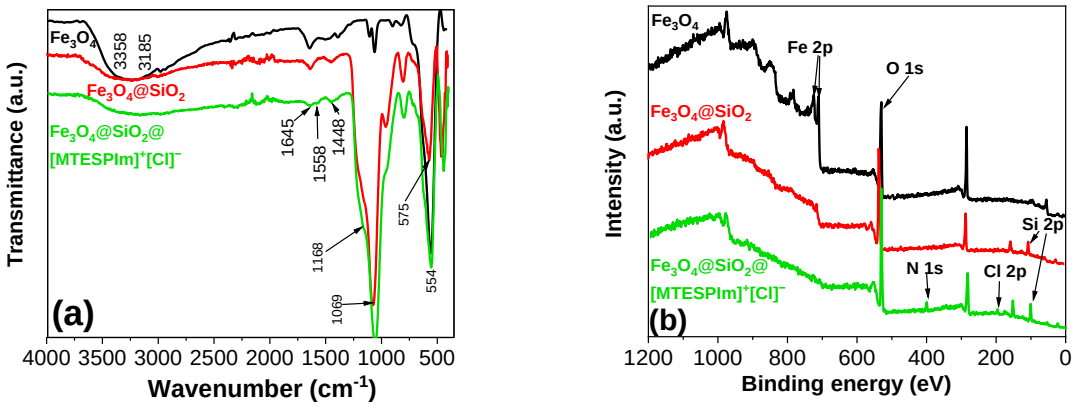

Fig. 3 (a) FTIR and (b)XPS spectra of Fe_3O_4 (black), Fe_3O_4@SiO_2 (red) and Fe_3O_4@SiO_2@$[MTESPIm]^+[Cl]^-$ (green)

More information allowed us to confirm the formation of the desired Fe_3O_4@SiO_2@$[MTESPIm]^+[Cl]^-$. The XPS spectra (Fig. 3b) confirms the FTIR data about the chemical compositions of all three nanoparticles. For example, photoelectron lines representing Fe 2p and O 1 s at 725/710 and 533 eV respectively can be observed in the survey spectra of all three nanoparticles (Sun et al. 2007). Furthermore, the spectra of the Fe_3O_4@SiO_2 is clearly different from that of the Fe_3O_4 with the presence of the extra photoelectron line representing Si 2p at 106 eV, confirming that SiO_2 has been chemisorbed onto the Fe_3O_4. Moreover, the spectra of the Fe_3O_4@SiO_2@$[MTESPIm]^+[Cl]^-$ (Fig. 3b (green)) also contains the Si 2p photoelectron line in addition to those of the N 1s, C 1s and Cl 2p at 400, 284.8 and 199 eV respectively, confirming the linkage of the ionic liquid to the Fe_3O_4@SiO_2 (Sun et al. 2007; Korin, Froumin, and Cohen 2017). The photoelectron lines at 284.8 eV (characteristic of the C 1s) in the spectra of all nanoparticles; Fe_3O_4, Fe_3O_4@SiO_2 and the Fe_3O_4@SiO_2@$[MTESPIm]^+[Cl]^-$ nanoparticles is attributed to adventitious carbon (Munho Kim et al. 2017; Miller, Biesinger, and McIntyre 2002).

The difference in surface compositions of the nanoparticles was further highlighted by the different weight loss patterns exhibited by the different nanoparticles in the TGA thermogram (Fig. 4). The weight loss of 4 % for the Fe_3O_4 nanoparticle between 180 and 570 °C was attributed to the loss of trapped water molecules in the Fe_3O_4 lattice and perhaps adventitious carbon as well (Khoobi et al. 2015). Expectedly, the silica coated Fe_3O_4 nanoparticles (Fe_3O_4@SiO_2) remained stable losing only 3 % in the entire experimental temperature range. The ionic liquid-modified silica coated Fe_3O_4 nanoparticles (Fe_3O_4@SiO_2@$[MTESPIm]^+[Cl]^-$) lost only 9 % of its weight attributed to the decomposition of the ionic liquid coating (Xu et al. 2013). The surface coverage of the ionic liquid coating on the Fe_3O_4@SiO_2 was found to be approximately 2 molecules/nm^2.

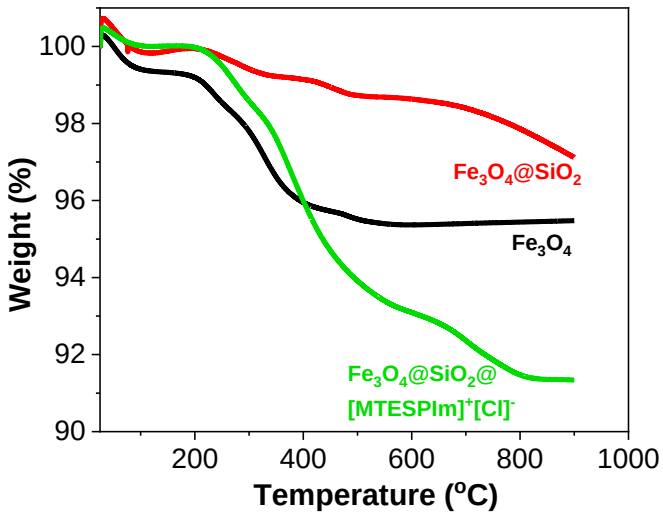

Fig. 4 TGA thermograms for Fe_3O_4 (black), silica coated Fe_3O_4 (red) and ionic liquid-modified silica coated Fe_3O_4 nanoparticles (green) (Atmosphere: nitrogen, heating rate: 10 °C/min)

Under the electron microscope, the Fe_3O_4 are spherical and aggregated particles with an average size of 13.5±2.8 nm (Figs. 5a and b). Aggregation of bare Fe_3O_4 nanoparticles is not uncommon and it has been explained that bare Fe_3O_4 particles aggregate in order to reduce their surface energy (Ditsch et al. 2005). The difference between the particle diameters obtained after analyses of the x-ray diffractogram (10.0±0.3 nm) and micrograph (13.5±2.8 nm) of Fe_3O_4 was attributed to error associated with manual sizing of the particles from the TEM micrograph. As expected, the $Fe_3O_4@SiO_2$ (Fig. 5c) and $Fe_3O_4@SiO_2@[MTESPIm]^+[Cl]^-$ particles (Fig. 5e) are bigger than the Fe_3O_4 with average sizes of 19.3±3.0 (Fig. 5d) and 18.5±3.1 nm (Fig. 5f) respectively, noting that these diameters are identical considering their errors. The aggregation observed for the $Fe_3O_4@SiO_2$ (Fig. 5c) particles has been attributed to the increase in ionic strength of the reaction medium as a result of the hydrolysis and condensation of the TEOS units (Philipse, Van Bruggen, and Pathmamanoharan 1994). On the other hand, aggregation observed for the $Fe_3O_4@SiO_2@[MTESPIm]^+[Cl]^-$ particles (Fig. 5e) may have been caused by intermolecular electrostatic attraction between surfaces bearing the ionic liquid. Based on the sizes of the Fe_3O_4 and the $Fe_3O_4@SiO_2$, the average thickness of the silica layer, which appear as grey fringes in the micrograph of the $Fe_3O_4@SiO_2$ (Fig. 5c) will have been about 6 nm.

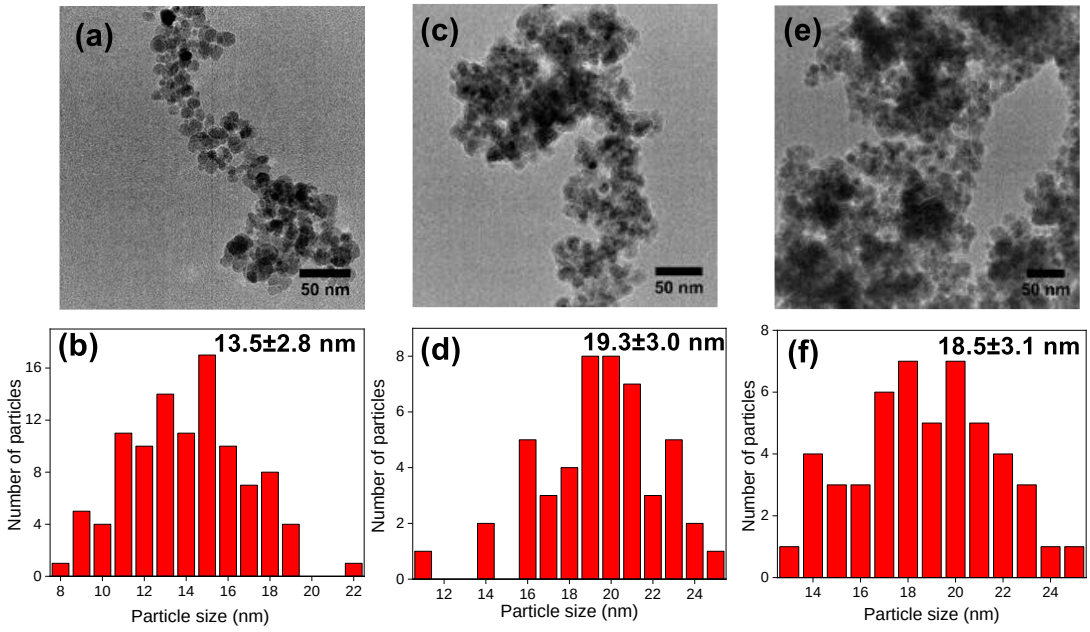

Fig. 5 (a,c,e) Transmission electron micrographs of (a) Fe_3O_4 (c) silica coated Fe_3O_4 and (e) ionic liquid-modified silica coated Fe_3O_4 nanoparticles, (b,d,f) Histograms showing size distribution of (b) Fe_3O_4 (d) silica coated Fe_3O_4 and (f) ionic liquid-modified silica coated Fe_3O_4 nanoparticles.

The observed particle diameters indicated that all three nanoparticles are superparamagnetic (being less than 20 nm) (Wahajuddin, A. and Arora 2012; Neamtu and Verga 2011). Indeed, this inference was confirmed from the magnetization curves (Fig. 6a) obtained after SQUID characterization, where all three nanoparticles had low coercivities (Mahdavian and Mirrahimi 2010; Salviano et al. 2018) (Fe_3O_4 = 18, $Fe_3O_4@SiO_2$ = 21 and

Fe_3O_4@SiO_2@[MTESPIm]$^+$[Cl]$^-$ = 22 Oe) (Fig. 6b). Expectedly, the Fe_3O_4 had the highest magnetization saturation (M_s) value of 77.60±0.10 emu/g. The M_s of the Fe_3O_4@SiO_2 and the Fe_3O_4@SiO_2@[MTESPIm]$^+$[Cl]$^-$ are not significantly different with values of 50.99±0.01 and 50.30±0.10 emu/g respectively, showing that the magnetic response of the Fe_3O_4@SiO_2 is not significantly reduced after the surface modification. The lower M_s for Fe_3O_4@SiO_2 and Fe_3O_4@SiO_2@[MTESPIm]$^+$[Cl]$^-$ is attributed to the surface modifications by non-magnetic materials – silica and the ionic liquid ([MTESPIm]$^+$[Cl]$^-$) respectively (Chen et al. 2014). Notwithstanding, the nanoparticle Fe_3O_4@SiO_2@[MTESPIm]$^+$[Cl]$^-$ can be quickly separated from an aqueous solution in about 1 min (Fig. 6a inset).

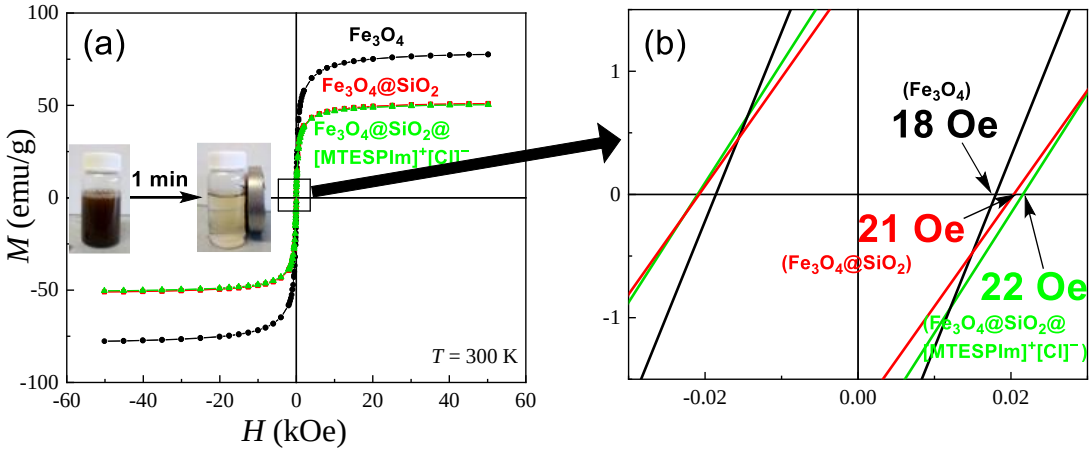

Fig. 6 (a) Magnetization curves for Fe_3O_4 (black), silica coated Fe_3O_4 (Fe_3O_4@SiO_2) (red) and ionic liquid-modified silica coated Fe_3O_4 nanoparticles (Fe_3O_4@SiO_2@[MTESPIm]$^+$[Cl]$^-$) (green) (Inset: separation of Fe_3O_4@SiO_2@[MTESPIm]$^+$[Cl]$^-$ from an aqueous solution using a magnet). (b) Expanded magnetization curve showing coercivities of Fe_3O_4 (black), Fe_3O_4@SiO_2 (red) and Fe_3O_4@SiO_2@[MTESPIm]$^+$[Cl]$^-$ (green).

Control study.

Prior to the investigation of the optimum conditions for Ag^+ removal by the Fe_3O_4@SiO_2@[MTESPIm]$^+$[Cl]$^-$, it was necessary to establish the ionic liquid; [MTESPIm]$^+$[Cl]$^-$ as the agent responsible for the Ag^+ removal. Therefore, the Ag^+ removal efficiencies of the nanoparticles; Fe_3O_4, Fe_3O_4@SiO_2 and Fe_3O_4@SiO_2@[MTESPIm]$^+$[Cl]$^-$ were measured by contacting 20 mg of each nanoparticle with 10 mL aqueous solution containing 1 mgL^{-1} Ag^+ at pH 1 and at room temperature.

The Ag^+ removal by the three nanoparticles increased in the order; Fe_3O_4 (3.4±0.6 %) < Fe_3O_4@SiO_2 (5.8±1.5 %) < Fe_3O_4@SiO_2@[MTESPIm]$^+$[Cl]$^-$ (94.4±0.4 %), with Fe_3O_4@SiO_2@[MTESPIm]$^+$[Cl]$^-$ demonstrating the highest removal efficiency (Fig. 7). The quantitative removal of Ag^+ by the Fe_3O_4@SiO_2@[MTESPIm]$^+$[Cl]$^-$ may be attributed to the preferential binding of the soft *N*- donor in the ionic liquid; [MTESPIm]$^+$[Cl]$^-$ to the soft Ag^+ acceptor

(Pearson 1968). Going forward, the nanoparticle Fe_3O_4@SiO_2@$[MTESPIm]^+[Cl]^-$ was employed for the investigation of the optimum conditions for the removal of Ag^+.

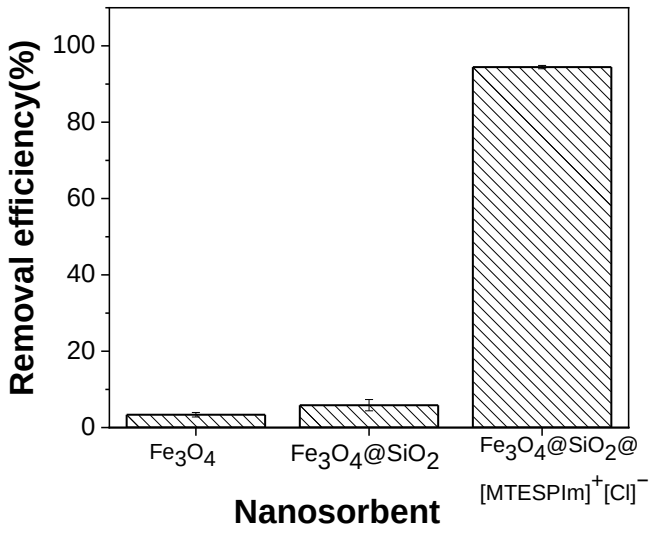

Fig. 7 Extraction efficiencies of Fe_3O_4, silica coated Fe_3O_4 nanoparticles (Fe_3O_4@SiO_2) and ionic liquid-modified silica coated Fe_3O_4 nanoparticles (Fe_3O_4@SiO_2@$[MTESPIm]^+[Cl]^-$) for Ag^+ extraction from aqueous solution. (conditions: $[Ag^+]_o$ = 1 mgL^{-1}, volume = 10 mL, pH = 1.0, contact time = 45 min, temperature = RT, nanosorbent dose = 20 mg).

Adsorption isotherms.

Figs. 8a-c display the sorption data plotted against Langmuir, Freundlich and Temkin isotherms after undertaking the relevant calculations. It can be observed that the Langmuir isotherm provided the best fit, with an R^2 value of 0.87 compared to 0.48 for Freundlich and 0.32 for Temkin (Table 1). This indicates that Ag^+ removal proceeded predominantly *via* chemisorption with the formation of a monolayer on $[MTESPIm]^+[Cl]^-$, with a saturation capacity of 23.69 mg/g. This agrees with Fig. 7 where the removal of Ag^+ onto Fe_3O_4 and Fe_3O_4@SiO_2 was comparatively much lower than $[MTESPIm]^+[Cl]^-$ on Fe_3O_4@SiO_2 and therefore suggests that the majority of Ag^+ sorption was with the ionic liquid. This therefore provides evidence that $[MTESPIm]^+[Cl]^-$ on Fe_3O_4@SiO_2 is a potentially reusable agent for Ag^+ removal.

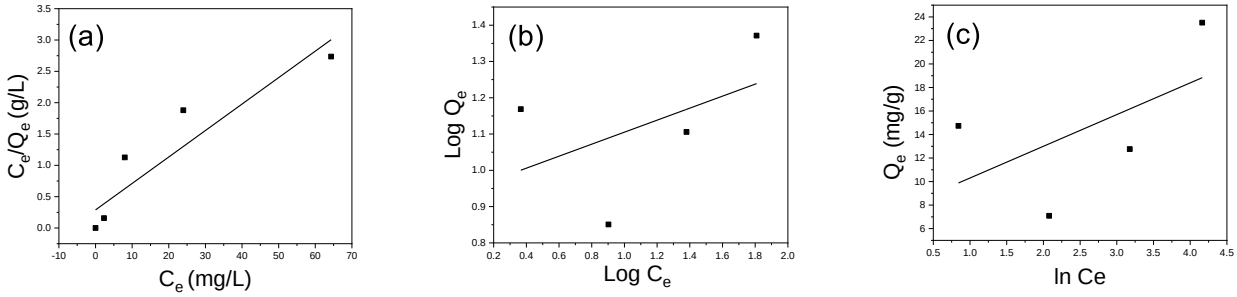

Fig. 8 (a) Langmuir, (b) Freundlich and (c) Temkin sorption isotherm plots for the removal of Ag^+ by the ionic liquid-modified silica coated Fe_3O_4 nanosorbent (pH = 3, time = 15 min, nanosorbent dose = 10 mg)

Table 1. Langmuir, Freundlich and Temkin isotherm parameters for the removal of Ag^+ by the ionic liquid-modified silica coated Fe_3O_4 nanosorbent (Fe_3O_4@SiO_2@$[MTESPIm]^+[Cl]^-$)

Langmuir			**Freundlich**			**Temkin**		
Q_m (mg/g)	K_L (L/mg)	R^2	K_F (mg/g)	n	R^2	B (J/mol)	A_T (L/g)	R^2
23.69	0.15	0.87	8.70	6.04	0.48	2.70	16.80	0.32

Effects of initial pH, contact time and nanosorbent dose on the efficiency and selectivity of removal Ag^+ by the nanosorbent; Fe_3O_4@SiO_2@$[MTESPIm]^+[Cl]^-$.

The effect of some conditions (including initial pH, contact time and nanosorbent dose) on the removal efficiency and selectivity of the nanosorbent; Fe_3O_4@SiO_2@$[MTESPIm]^+[Cl]^-$ for Ag^+ removal from aqueous solutions also containing competing ions (Cu^{2+} and Pb^{2+}) were investigated by contacting the nanosorbent with 10 mL of aqueous solutions containing ca. 2 mgL^{-1} each of Cu^{2+}, Ag^+ and Pb^{2+}. The choice of Cu^{2+} and Pb^{2+} as competing ions was informed by the knowledge that Ag^+, usually coexists with Cu^{2+} and Pb^{2+} in ores and mine tailings, for example (Crane et al. 2017). Also, it was stated that very low concentrations of Ag^+, Cu^{2+} and Pb^{2+} was employed in this study because Ag^+, typically exists in very low concentrations in potential Ag^+ repositories of interest.

Effect of initial pH.

The pH is an important parameter usually investigated in metal removal studies since metal extraction efficiencies have usually been found to be dependent upon pH (Abdolmohammad-Zadeh and Javan 2015; Karimi et al. 2012). In this study, the effect of selectivity for and extraction efficiency of Ag^+ was investigated by varying the pH of the

mixed metal aqueous solution from 1 to 5. This pH range was chosen since the efficiency of the nanosorbent at low pH was of particular interest because of low pH environments the nanosorbent may be applied to. Interestingly, it was observed that the extraction efficiency of Ag^+ by the nanosorbent; $Fe_3O_4@SiO_2@[MTESPIm]^+[Cl]^-$ was dependent on pH. The highest extraction efficiency for Ag^+ (99.2±0.8 %) was obtained at pH 3 (Fig. 9a). Similar studies have reported excellent extraction efficiencies at this pH (Daubinet and Kaye 2002; Abdolmohammad-Zadeh and Javan 2015). The quantitative removal of Ag^+ at this pH (pH 3) has been explained by the hard soft acid base (HSAB) rule (Pearson 1968). This explanation also helps to understand the quantitative recoveries of Ag^+ at lower pH (pH 1 = 95.5±0.7 %, pH 2 = 97.7±0.7 %) (Fig. 9a). Furthermore, observation of quantitative extraction efficiencies of Ag^+ at very low pH indicates that the nanosorbent is likely to be stable at low pH.

The selectivity for Ag^+ over Cu^{2+} and Pb^{2+} by the nanosorbent was also observed to be pH dependent. The highest selectivity for Ag^+ over both Cu^{2+} and Pb^{2+} was observed at pH 3 ($K_{Ag^+/Cu^{2+}}$ = 2272.3 and $K_{Ag^+/Pb^{2+}}$ = 928.7) (Fig. 9b). It can be observed that the selectivity factor of the adsorbent for Cu^{2+} was higher than that for Pb^{2+} over the pH range investigated. It is unclear why this was observed. In hard/soft terms Cu^{2+} is softer than Pb^{2+}, therefore the selectivity for Ag^+ over Pb^{2+} should be higher than over Cu^{2+} and not the other way around as observed. Other factors such as differential removal by precipitation as Pb and Cu chlorides or electrostatic attraction of the aqua ions; $Pb_4(OH)_4^{4+}$ and $Cu(H_2O)_6]^{2+}$ to the Cl^- in the nanoparticle are unlikely explanations as they both form chlorides and aqua ions readily. It might be related to the average pore size of the nanoparticles (the ionic radius of Pb^{2+} is bigger than Cu^{2+} (1.27 vs 0.72 Å), but this couldn't be verified as the pore size of the nanoparticles were not measured. Summarily, the highest extraction efficiency and highest selectivity of Ag^+ were obtained the nanosorbent; $Fe_3O_4@SiO_2@[MTESPIm]^+[Cl]^-$ were obtained at pH 3.

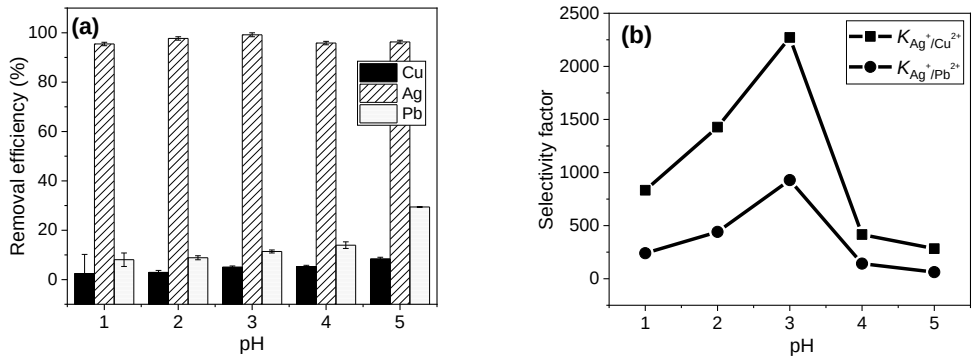

Fig. 9 Effect of pH on (a) efficiency and (b) selectivity of Ag^+ removal from simulated mixed metal aqueous solution by the ionic liquid-modified silica coated Fe_3O_4 nanosorbent ($[M^{n+}]$ = 2 mgL^{-1}, volume = 10 mL, contact time = 2 h, temperature = RT, nanosorbent dose = 10 mg)

Effect of contact time.

The optimum contact time for the extraction of Ag^+ by the nanosorbent; $Fe_3O_4@SiO_2@[MTESPIm]^+[Cl]^-$ was investigated by varying the contact time from 0 to 90 min. A duration of 0 min refers to the situation where the nanoparticle is separated immediately after the nanosorbent had been contacted with the mixed metal aqueous solution. Usually, the magnetic separation of the nanosorbent occurs in about 1 min.

The extraction efficiency showed no significant difference across the contact time; 15-90 min, with the highest and lowest extraction efficiencies being 96.1±0.7 % (75 min) and 94.9±0.7 % (0 min) respectively (Fig. 10a). This observation was attributed to the availability of enough sites on the surface of the nanosorbent for the removal of Ag^+ with a rapid reactivity (noting even at 0 minutes 94.9% of Ag^+ was removed) (Lasheen et al. 2014; Beigzadeh and Moeinpour 2016).

The selectivity factor of Ag^+ over the interfering ions (Cu^{2+} and Pb^{2+}) worsens over an increase in the contact time. The highest selectivity factor for Ag^+ over Cu^{2+} and Pb^{2+} were observed at 0 and 15 min respectively (Fig. 10b), with the implication that selective Ag^+ removal is favourable for the least duration possible suggesting a kinetically controlled selectivity. The lowest selectivity factor of Ag^+ over Cu^{2+} and Pb^{2+} were observed at 90 min, indicating that exchange of metals may be occurring in line with a thermodynamic equilibrium being reached, thus allowance for a lengthy contact time reduces the selective extraction of Ag^+.

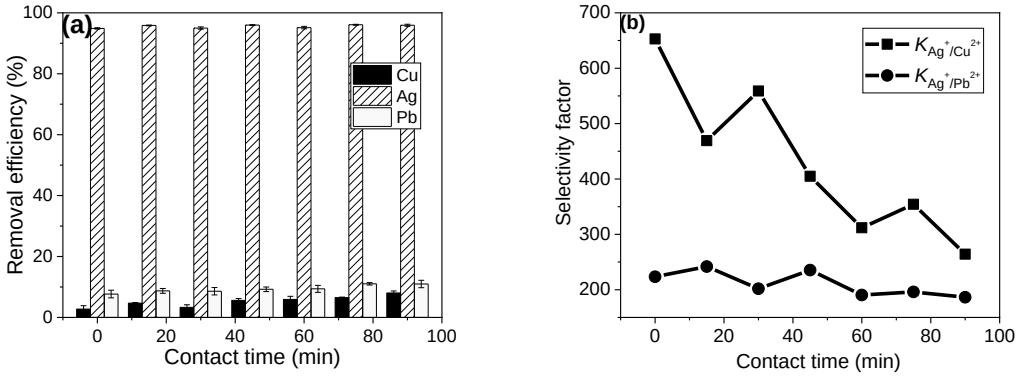

Fig. 10 Effect of contact time on (a) efficiency and (b) selectivity on Ag^+ removal from simulated mixed metal aqueous solution using the ionic liquid-modified silica coated Fe_3O_4 nanosorbent (Conditions: $[M^{n+}]$ = 2 mgL^{-1}, volume = 10 mL, pH = 1.30, temperature = RT, nanosorbent dose = 10 mg).

Effect of nanosorbent dose.

In order to develop an efficient and cost-effective metal extraction system, determination of the optimum dose of the nanosorbent needed is important. Therefore, the effect of nanosorbent ($Fe_3O_4@SiO_2@[MTESPIm]^+[Cl]^-$) dose on efficiency and selectivity of Ag^+ was investigated by varying the amount of the nanosorbent contacted with the mixed metal solution from 5 to 80 mg for 45 min. Unsurprisingly, the extraction efficiency for Ag^+ extraction increased with

increasing nanosorbent dose (Fig. 11a). The lowest and highest extraction efficiencies for Ag^+ were observed at the lowest and highest amounts of nanosorbent used (87.0±0.3 % at 5 mg and 99.5±0.1 % for 80 mg). The increase of Ag^+ extraction efficiency with increasing nanosorbent dosage used is of course due to the increase in the number of sites on nanosorbent available for binding Ag^+. The lowest efficiency observed (87.0±0.3 %) is better than the 85 % extraction efficiency reported in the literature (Abdolmohammad-Zadeh and Javan 2015) where a greater amount of a similar nanosorbent was used. This difference was attributed to the higher surface area of the nanosorbent in contact with the aqueous solution in this study compared with that in the literature (Abdolmohammad-Zadeh and Javan 2015), as they confined their nanosorbent in a syringe while in this study, the nanosorbent was dispersed in the mixed metal aqueous solution.

The selectivity factor of Ag^+ over the interfering ions (Cu^{2+} and Pb^{2+}) was also found to be dependent on nanosorbent dose. From Fig. 11b, the highest selectivity for Ag^+ over the interfering ions ($K_{Ag^+/Cu^{2+}}$ = 4119.9 and $K_{Ag^+/Pb^{2+}}$ = 2250.9) was obtained with the highest nanosorbent dose used (80 mg), although the reasons for this remain unclear. Therefore, in practical terms, the highest purity of Ag^+ can be recovered from a mixed metal solution containing the ion alongside Cu^{2+} and Pb^{2+} by using as much of the nanosorbent; $Fe_3O_4@SiO_2@[MTESPIm]^+[Cl]^-$ as would be commercially possible.

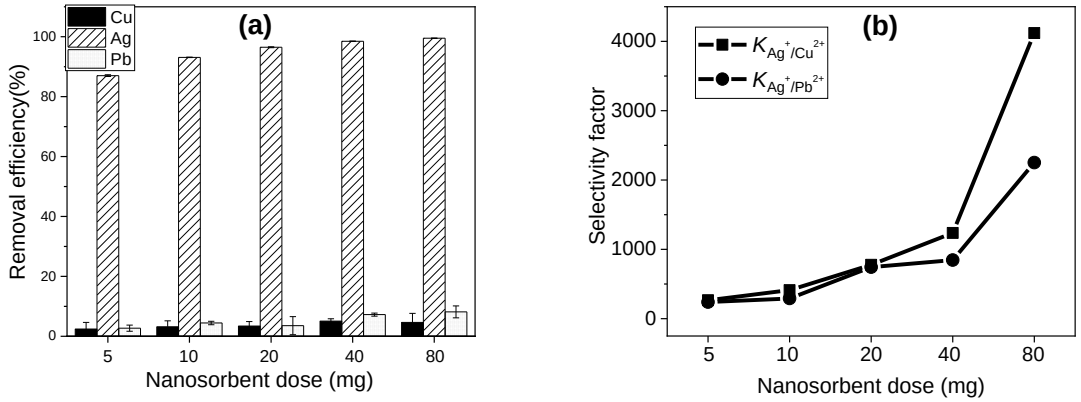

Fig. 11 Effect of nanosorbent dose on (a) efficiency and (b) selectivity on Ag^+ removal from simulated mixed metal aqueous solution by the nanosorbent; $Fe_3O_4@SiO_2@[MTESPIm]^+[Cl]^-$ (conditions: $[M^{n+}]$ = 2 mgL^{-1}, volume = 10 mL, pH = 1.30, contact time = 45 min, temperature = RT).

Effect of type of stripping agents.

Recovery of the extracted metal ion is an important factor in studies on metal recycling. Furthermore, the choice of an efficient metal recovery (or stripping) agent and establishment of optimum recovery conditions is important in metal recycling studies. Therefore, the effect of the type of the stripping agent on the efficiency of Ag^+ recovery was investigated by contacting aqueous solutions of three different types of stripping agents – HCl (0.6 and 3 M), HNO_3 (0.6 and 3 M) and thiourea (0.6 M) with Ag^+ loaded nanosorbent - $Fe_3O_4@SiO_2@[MTESPIm]^+[Cl]^-$, noting that 3 M

thiourea could not be prepared due to the limited solubility in water. The choice of HCl and thiourea for this study was informed by previous work which reported excellent stripping efficiencies of Ag^+ by these stripping agents (Abdolmohammad-Zadeh and Javan 2015; Vojoudi et al. 2017; Kazemi, Haji Shabani, and Dadfarnia 2015; Shimojo and Goto 2004).

Stripping of Ag^+ from the Ag^+-impregnated nanosorbent was found to be dependent on the type of stripping agent. Predictably, the highest % SE (85.4±1.3 %) was observed for 0.6 M thiourea and this was attributed to the preference of the soft *S*- donor atom in thiourea for the soft Ag^+ acceptor (Fig. 12) (Pearson 1968). Presumably, a higher % SE could be observed at higher thiourea concentration. Interestingly, 3 M, HCl as found to strip more Ag^+ than HNO_3 of the same concentration (HCl = 59.5±5.5 % vs HNO_3 = 30.9±3.4 %). This could be attributed to the formation of the anionic complex – $AgCl_2^-$ at high Cl^- concentrations (Abdolmohammad-Zadeh and Javan 2015). The % SE observed for both acids at 0.6 M are identical considering their errors. Generally, an increase in the concentration of the stripping agent (excluding thiourea) resulted in an increase in % SE, but thiourea was the agent of choice.

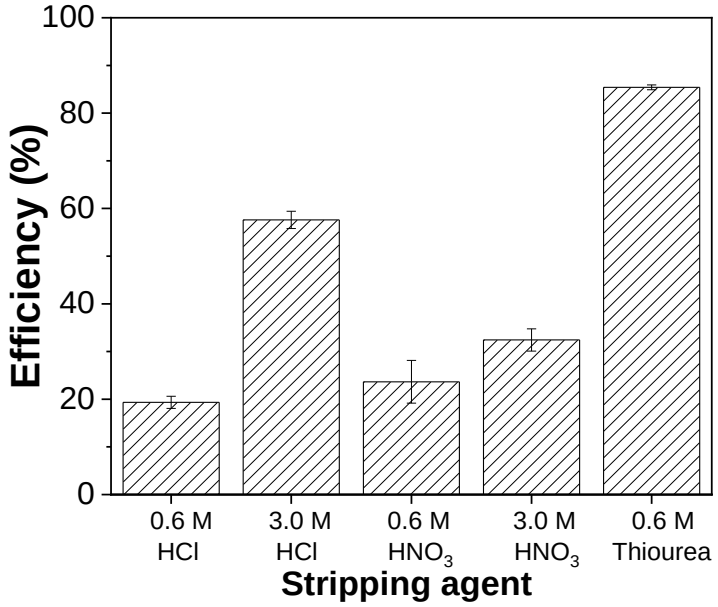

Fig. 12 Relationship between stripping agent type and concentration in the stripping of Ag^+ from impregnated Fe_3O_4@SiO_2@$[MTESPIm]^+[Cl]^-$ nanosorbent (volume of acid = 5 mL, contact time = 1 h, temperature = RT).

Conclusion

Surface functionalized magneto-responsive nanoparticles are a new class of materials which have received much interest in recent years for their potential utility as next generation agents for the recovery of metal(loid)s from the aqueous phase. Herein the ligand $[MTESPIm]^+[Cl]^-$ on Fe_3O_4@SiO_2 was prepared and characterized using FTIR, XPS, TGA, TEM and SQUID which confirmed that the nanomaterial exhibited a well constrained composition, physical structure and particle size distribution, in addition to a high saturation magnetism. SQUID analysis recorded a

magnetic saturation of 50.30±0.10 emu/g and thereby indicating that the nanomaterial is highly amenable for its transport and recovery from the aqueous phase using an externally applied magnetic field. Characterization using TGA recorded a surface coverage of the ionic liquid coating on the $Fe_3O_4@SiO_2$ of approximately 2 molecules/nm^2. The $[MTESPIm]^+[Cl]^-$ on $Fe_3O_4@SiO_2$ was found to be highly efficient and selective for Ag^+ removal from solutions also containing Cu^{2+} and Pb^{2+}, with optimum efficiency and selectivity recorded at pH 3, with an exposure time of between 0-15 minutes. Analysis of the Langmuir isotherm indicated a monolayer coverage of Ag^+ on the nanosorbent, with a saturation capacity of 23.69 mg/g. Thiourea (0.6 M) was the most effective Ag^+ stripping agent, which is attributed to the preference of the soft *S*- donor atom in thiourea for the soft Ag^+ acceptor. Overall, the results confirm that $[MTESPIm]^+[Cl]^-$ on $Fe_3O_4@SiO_2$ is a highly effective, versatile and selective agent for the removal of Ag from the aqueous phase and is therefore well suited for multiple future applications in both waste water treatment and mining sectors.

Funding. The authors would like to thank The UK Commonwealth Scholarship Commission for funding the research under grant number NGCS-2015-448.

Compliance with ethical standards

Conflict of Interest. The authors declare that they have no conflict of interest.

References

Abbas, Mohamed, B. Parvatheeswara Rao, Md Nazrul Islam, S. M. Naga, Migaku Takahashi, and Cheolgi Kim. 2014. "Highly Stable-Silica Encapsulating Magnetite Nanoparticles (Fe 3O4/SiO2) Synthesized Using Single Surfactantless- Polyol Process." *Ceramics International* 40 (1 PART B): 1379–85. https://doi.org/10.1016/j.ceramint.2013.07.019.

Abdolmohammad-Zadeh, Hossein, and Zahra Javan. 2015. "Silica-Coated Mn3O4 Nanoparticles Coated with an Ionic Liquid for Use in Solid Phase Extraction of Silver(I) Ions Prior to Their Determination by AAS." *Microchimica Acta* 182: 1447–56. https://doi.org/10.1007/s00604-015-1468-x.

Ahlatcı, F, E Koç, E Y Yazici, O Celep, and H Deveci. 2016. "Sulphide Precipitation of Gold and Silver from Thiosulphate Leach Solutions." *XV. International Mineral Processing Symposium and Exhibition (IMPS)*, no. October: 750–60.

Avarmaa, Katri, Lassi Klemettinen, Hugh O'Brien, and Pekka Taskinen. 2019. "Urban Mining of Precious Metals via Oxidizing Copper Smelting." *Minerals Engineering* 133 (March): 95–102. https://doi.org/10.1016/j.mineng.2019.01.006.

Azgomi, Naghmeh, and Masoud Mokhtary. 2015. “Nano-Fe3O4@SiO2 Supported Ionic Liquid as an Efficient Catalyst for the Synthesis of 1,3-Thiazolidin-4-Ones under Solvent-Free Conditions.” *Journal of Molecular Catalysis A: Chemical* 398: 58–64. https://doi.org/10.1016/j.molcata.2014.11.018.

Banaei, Alireza, Hossein Vojoudi, Soheyla Karimi, Shahriyar Bahar, and Eslam Pourbasheer. 2015. “Synthesis and Characterization of New Modified Silica Coated Magnetite Nanoparticles with Bisaldehyde as Selective Adsorbents of Ag(i) from Aqueous Samples.” *RSC Advances* 5 (101): 83304–13. https://doi.org/10.1039/c5ra11765h.

Beigzadeh, Parisa, and Farid Moeinpour. 2016. “Fast and Efficient Removal of Silver (I) from Aqueous Solutions Using Aloe Vera Shell Ash Supported Ni0.5Zn0.5Fe2O4magnetic Nanoparticles.” *Transactions of Nonferrous Metals Society of China (English Edition)* 26 (8): 2238–46. https://doi.org/10.1016/S1003-6326(16)64341-8.

Butterman, By W C, and H E Hilliard. 2005. “Mineral Commodity Profiles: Silver.” Virginia. https://doi.org/https://pubs.usgs.gov/of/2004/1251/2004-1251.pdf.

Chen, Jing, Yuzhi Wang, Xueqin Ding, Yanhua Huang, and Kaijia Xu. 2014. “Magnetic Solid-Phase Extraction of Proteins Based on Hydroxy Functional Ionic Liquid-Modified Magnetic Nanoparticles.” *Analytical Methods* 6 (20): 8358–67. https://doi.org/10.1039/c4ay01786b.

Crane, R. A., D. E. Sinnett, P. J. Cleall, and D. J. Sapsford. 2017. “Physicochemical Composition of Wastes and Co-Located Environmental Designations at Legacy Mine Sites in the South West of England and Wales: Implications for Their Resource Potential.” *Resources, Conservation and Recycling* 123: 117–34. https://doi.org/10.1016/j.resconrec.2016.08.009.

Daubinet, André, and Perry T. Kaye. 2002. “Designer Ligands. VIII. Thermal and Microwave-Assisted Synthesis of Silver(I)-Selective Ligands.” *Synthetic Communications* 32 (20): 3207.

Ditsch, Andre, Paul E. Laibinis, Daniel I.C. Wang, and T. Alan Hatton. 2005. “Controlled Clustering and Enhanced Stability of Polymer-Coated Magnetic Nanoparticles.” *Langmuir* 21 (13): 6006–18. https://doi.org/10.1021/la047057+.

Fan, Liren, Jiqing Song, Wenbo Bai, Shengping Wang, Ming Zeng, Xiaoming Li, Yang Zhou, Haifeng Li, and Haiwei Lu. 2016. “Chelating Capture and Magnetic Removal of Non-Magnetic Heavy Metal Substances from Soil.” *Scientific Reports* 6 (February): 1–9. https://doi.org/10.1038/srep21027.

Filippousi, Maria, Mavroeidis Angelakeris, Maria Katsikini, Eleni Paloura, Ilias Efthimiopoulos, Yuejian Wang, Demetris Zamboulis, and Gustaaf Van Tendeloo. 2014. “Surfactant Effects on the Structural and Magnetic Properties of Iron Oxide Nanoparticles.” *Journal of Physical Chemistry C* 118 (29): 16209–17. https://doi.org/10.1021/jp5037266.

Garkoti, Charu, Javaid Shabir, and Subho Mozumdar. 2017. “An Imidazolium Based Ionic Liquid Supported on

Fe3O4@SiO2 Nanoparticles as an Efficient Heterogeneous Catalyst for N-Formylation of Amines." *New Journal of Chemistry* 41 (17): 9291–98. https://doi.org/10.1039/c6nj03985e.

Hufschmid, Ryan, Hamed Arami, R. Matthew Ferguson, Marcela Gonzales, Eric Teeman, Lucien N. Brush, Nigel D. Browning, and Kannan M. Krishnan. 2015. "Synthesis of Phase-Pure and Monodisperse Iron Oxide Nanoparticles by Thermal Decomposition." *Nanoscale* 7 (25): 11142–54. https://doi.org/10.1039/c5nr01651g.

Jalilian, Rahil, and Alireza Taheri. 2018. "Synthesis and Application of a Novel Core-Shell-Shell Magnetic Ion Imprinted Polymer as a Selective Adsorbent of Trace Amounts of Silver Ions." *E-Polymers* 18 (2): 123–34. https://doi.org/10.1515/epoly-2017-0108.

Karimi, Mohammad Ali, Abdolhamid Hatefi-Mehrjardi, Sayed Zia Mohammadi, Alireza Mohadesi, Mohammad Mazloum-Ardakani, Asghar Askarpour Kabir, Maryam Kazemipour, and Najmeh Afsahi. 2012. "Solid Phase Extraction of Trace Amounts of Silver (I) Using Dithizone-Immobilized Alumina-Coated Magnetite Nanoparticles Prior to Determination by Flame Atomic Absorption Spectrometry." *International Journal of Environmental Analytical Chemistry* 92 (12): 1325–40. https://doi.org/10.1080/03067319.2011.563385.

Kazemi, Elahe, Ali Mohammad Haji Shabani, and Shayessteh Dadfarnia. 2015. "Synthesis and Characterization of a Nanomagnetic Ion Imprinted Polymer for Selective Extraction of Silver Ions from Aqueous Samples." *Microchimica Acta* 182 (5–6): 1025–33. https://doi.org/10.1007/s00604-014-1430-3.

Khoobi, Mehdi, Tayebeh Modiri Delshad, Mohsen Vosooghi, Masoumeh Alipour, Hosein Hamadi, Eskandar Alipour, Majid Pirali Hamedani, et al. 2015. "Polyethyleneimine-Modified Superparamagnetic Fe3O4 Nanoparticles: An Efficient, Reusable and Water Tolerance Nanocatalyst." *Journal of Magnetism and Magnetic Materials* 375: 217–26. https://doi.org/10.1016/j.jmmm.2014.09.044.

Kim, Minsik, Sohee Hwang, and Jong Sung Yu. 2007. "Novel Ordered Nanoporous Graphitic C3N4 as a Support for Pt-Ru Anode Catalyst in Direct Methanol Fuel Cell." *Journal of Materials Chemistry* 17 (17): 1656–59. https://doi.org/10.1039/b702213a.

Kim, Munho, Jung Hun Seo, Deyin Zhao, Shih Chia Liu, Kwangeun Kim, Kangmook Lim, Weidong Zhou, Edo Waks, and Zhenqiang Ma. 2017. "Transferrable Single Crystalline 4H-SiC Nanomembranes." *Journal of Materials Chemistry C* 5 (2): 264–68. https://doi.org/10.1039/c6tc04480h.

Korin, Efrat, Natalya Froumin, and Smadar Cohen. 2017. "Surface Analysis of Nanocomplexes by X-Ray Photoelectron Spectroscopy (XPS)." *ACS Biomaterials Science and Engineering* 3 (6): 882–89. https://doi.org/10.1021/acsbiomaterials.7b00040.

Lasheen, M. R., I. Y. El-Sherif, Dina Y. Sabry, S. T. El-Wakeel, and M. F. El-Shahat. 2014. "Removal and Recovery of Cr (VI) by Magnetite Nanoparticles." *Desalination and Water Treatment* 52 (34–36): 6464–73. https://doi.org/10.1080/19443994.2013.822158.

519 Mahdavian, Ali Reza, and Monir Al Sadat Mirrahimi. 2010. “Efficient Separation of Heavy Metal Cations by
520 Anchoring Polyacrylic Acid on Superparamagnetic Magnetite Nanoparticles through Surface Modification.”
521 *Chemical Engineering Journal* 159 (1–3): 264–71. https://doi.org/10.1016/j.cej.2010.02.041.

522 Miller, D. J., M. C. Biesinger, and N. S. McIntyre. 2002. “Interactions of CO2 and CO at Fractional Atmosphere
523 Pressures with Iron and Iron Oxide Surfaces: One Possible Mechanism for Surface Contamination?” *Surface*
524 *and Interface Analysis* 33: 299–305. https://doi.org/10.1002/sia.1188.

525 Naka, K., A. Narita, H. Tanaka, Y. Chujo, M. Morita, T. Inubushi, I. Nishimura, et al. 2008. “Biomedical Applications
526 of Imidazolium Cation-Modified Iron Oxide Nanoparticles.” *Polymers for Advanced Technologies* 19: 1421–
527 29. https://doi.org/10.1002/pat.1218.

528 Neamtu, J., and N. Verga. 2011. “Magnetic Nanoparticles for Magneto-Resonance Imaging and Targeted Drug
529 Delivery.” *Digest Journal of Nanomaterials and Biostructures* 6 (3): 969–78.

530 Ozkaya, T., A. Baykal, H. Kavas, Y. Köseoğlu, and M. S. Toprak. 2008. “A Novel Synthetic Route to Mn3O4
531 Nanoparticles and Their Magnetic Evaluation.” *Physica B: Condensed Matter* 403 (19–20): 3760–64.
532 https://doi.org/10.1016/j.physb.2008.07.002.

533 Pearson, Ralph G. 1968. “Hard and Soft Acids and Bases, HSAB, Part 1: Fundamental Principles.” *Journal of*
534 *Chemical Education* 45 (9): 581. https://doi.org/10.1021/ed045p581.

535 Philipse, Albert P., Michel P.B. Van Bruggen, and Chellapah Pathmamanoharan. 1994. “Magnetic Silica Dispersions:
536 Preparation and Stability of Surface-Modified Silica Particles with a Magnetic Core.” *Langmuir* 10 (1): 92–99.
537 https://doi.org/10.1021/la00013a014.

538 Puig, J., C. E. Hoppe, L. A. Fasce, C. J. Pérez, Y. Piñeiro-Redondo, M. Bañobre-López, M. A. López-Quintela, J.
539 Rivas, and R. J.J. Williams. 2012. “Superparamagnetic Nanocomposites Based on the Dispersion of Oleic Acid-
540 Stabilized Magnetite Nanoparticles in a Diglycidylether of Bisphenol A-Based Epoxy Matrix: Magnetic
541 Hyperthermia and Shape Memory.” *Journal of Physical Chemistry C* 116: 13421–28.
542 https://doi.org/10.1021/jp3026754.

543 Qian, Liwei, Jiexuan Sun, Chen Hou, Jinfan Yang, Yongwei Li, Dan Lei, Miaoxiu Yang, and Sufeng Zhang. 2017.
544 “Immobilization of BSA on Ionic Liquid Functionalized Magnetic Fe3O4 Nanoparticles for Use in Surface
545 Imprinting Strategy.” *Talanta* 168 (January): 174–82. https://doi.org/10.1016/j.talanta.2017.03.044.

546 Sahan, Merve, Mehmet Ali Kucuker, Burak Demirel, Kerstin Kuchta, and Andrew Hursthouse. 2019. “Determination
547 of Metal Content of Waste Mobile Phones and Estimation of Their Recovery Potential in Turkey.” *International*
548 *Journal of Environmental Research and Public Health* 16 (5). https://doi.org/10.3390/ijerph16050887.

549 Sajjadifar, Sami, Mohammad Ali Zolfigol, and Farzaneh Tami. 2019. “Application of 1-Methyl Imidazole-Based Ionic
550 Liquid-Stabilized Silica-Coated Fe 3 O 4 as a Novel Modified Magnetic Nanocatalyst for the Synthesis of

Pyrano[2,3-d]Pyrimidines." *Journal of the Chinese Chemical Society* 66 (3): 307–15. https://doi.org/10.1002/jccs.201800171.

Salviano, Luciana Barbosa, Thays Michelle da Silva Cardoso, Gabriela Cordeiro Silva, Maria Sylvia Silva Dantas, and Angela de Mello Ferreira. 2018. "Microstructural Assessment of Magnetite Nanoparticles (Fe3O4) Obtained by Chemical Precipitation Under Different Synthesis Conditions." *Materials Research* 21 (2): 2–8. https://doi.org/10.1590/1980-5373-mr-2017-0764.

Seddon, Kenneth R, Annegret Stark, and María-josé Torres. 2000. "Influence of Chloride , Water , and Organic Solvents on the Physical Properties of Ionic Liquids *" 72 (12): 2275–87.

Shamsipur, Mojtaba, Beshare Hashemi, Sara Dehdashtian, Moslem Mohammadi, Mohammad Bagher Gholivand, Alessandra Garau, and Vito Lippolis. 2014. "Silver Ion Imprinted Polymer Nanobeads Based on a Aza-Thioether Crown Containing a 1,10-Phenanthroline Subunit for Solid Phase Extraction and for Voltammetric and Potentiometric Silver Sensors." *Analytica Chimica Acta* 852: 223–35. https://doi.org/10.1016/j.aca.2014.09.028.

Shimojo, Kojiro, and Masahiro Goto. 2004. "Solvent Extraction and Stripping of Silver Ions in Room-Temperature Ionic Liquids Containing Calixarenes." *Analytical Chemistry* 76 (17): 5039–44. https://doi.org/10.1021/ac049549x.

Sun, Yabin, Xiaobin Ding, Zhaohui Zheng, Xu Cheng, Xinhua Hu, and Yuxing Peng. 2007. "Surface Initiated ATRP in the Synthesis of Iron Oxide/Polystyrene Core/Shell Nanoparticles." *European Polymer Journal* 43: 762–72. https://doi.org/10.1016/j.eurpolymj.2006.10.021.

Taillades, G., and J. Sarradin. 2004. "Silver: High Performance Anode for Thin Film Lithium Ion Batteries." *Journal of Power Sources* 125 (2): 199–205. https://doi.org/10.1016/j.jpowsour.2003.07.004.

Virolainen, Sami, Mikko Tyster, Mika Haapalainen, and Tuomo Sainio. 2015. "Ion Exchange Recovery of Silver from Concentrated Base Metal-Chloride Solutions." *Hydrometallurgy* 152: 100–106. https://doi.org/10.1016/j.hydromet.2014.12.011.

Vojoudi, Hossein, Alireza Badiei, Alireza Banaei, Shahriyar Bahar, Soheyla Karimi, Ghodsi Mohammadi Ziarani, and Mohammad Reza Ganjali. 2017. "Extraction of Gold, Palladium and Silver Ions Using Organically Modified Silica-Coated Magnetic Nanoparticles and Silica Gel as a Sorbent." *Microchimica Acta* 184 (10): 3859–66. https://doi.org/10.1007/s00604-017-2414-x.

Wahajuddin, A. and Arora, S. 2012. "Superparamagnetic Iron Oxide Nanoparticles: Magnetic Nanoplatforms as Drug Carriers." *International Journal of Medicine* 7: 3445–71.

Wei, Yun, Yan Li, Ailin Tian, Yuntian Fan, and Xiong Wang. 2013. "Ionic Liquid Modified Magnetic Microspheres for Isolation of Heme Protein with High Binding Capacity." *Journal of Materials Chemistry B* 1 (15): 2066–71.

https://doi.org/10.1039/c3tb00576c.

Xu, Jiakun, Caixia Ju, Jun Sheng, Fang Wang, Quan Zhang, Guolong Sun, and Mi Sun. 2013. “Synthesis and Characterization of Magnetic Nanoparticles and Its Application in Lipase Immobilization.” *Bulletin of the Korean Chemical Society* 34 (8): 2408–12. https://doi.org/10.5012/bkcs.2013.34.8.2408.

Yang, Fei, Rui Shen, Yiming Long, Xiangyu Sun, Fei Tang, Qingyun Cai, and Shouzhuo Yao. 2011. “Magnetic Microsphere Confined Ionic Liquid as a Novel Sorbent for the Determination of Chlorophenols in Environmental Water Samples by Liquid Chromatography.” *Journal of Environmental Monitoring* 13 (2): 440–45. https://doi.org/10.1039/c0em00389a.

Yin, Xiaocui, Jian Long, Yu Xi, and Xubiao Luo. 2017. “Recovery of Silver from Wastewater Using a New Magnetic Photocatalytic Ion-Imprinted Polymer.” *ACS Sustainable Chemistry and Engineering* 5 (3): 2090–97. https://doi.org/10.1021/acssuschemeng.6b01871.

Zhou, Huacong, Liangrong Yang, Wei Li, Qinghui Shou, Peng Xu, Wensong Li, Fuchun Wang, Pinhua Yu, and Huizhou Liu. 2012. “Improving the Stability of Immobilized Penicillin G Acylase via the Modification of Supports with Ionic Liquids.” *Industrial and Engineering Chemistry Research* 51 (12): 4582–90. https://doi.org/10.1021/ie202745c.